

Mangafodipir Trisodium

MR

가?:

1

1, 2 . 2

: Mangafodipir trisodium (Mn - DPDP)

MR

,
: (n=20) (n=15) Mn - DPDP
T1 - MR .
, , ,
: (n=69) 가 44 (63.8%),
가 25 (36.2%) , 가 16 (23.2%),
가 38 (55.1%),
15 (21.7%) . (n=37) 가 36
(97.3%) , 1 (2.7%) ,
1 (2.7%) . MR
가 ,
: Mn - DPDP MR

MR Gadopentetate dimeglu - (5 - 8). Mn - DPDP
mine (Gd - DTPA) (1), (ring)
가 . 가 (,
Mangafodipir ,) 가 (6, 7).
trisodium (Mn - DPDP) Gd - DTPA
DPDP (dipyridoxyl diphosphate)가 , Mn - DPDP
가
(2 - 4). . Mn - DPDP
Mn - DPDP T1 - 15 - 20 4 가
가 , 24
가 (9 - 11).
T1 - (12,
13),

가

가

(flushing)

. Mn - DPDP

T2 -

, Mn - DPDP

T2 -

T2

20

15

Mn - DPDP

30 () MR

12

()

2

가

CT

MR

CT

MR

(confidence

CT

rating)

1,

2,

가

3,

4,

5

11 ,

9 ,

61

12 ,

3 ,

58

7 (n=25),

가

4

4

3

5 (n=14),

3 (n=15),

3 (n=10),

가

0,

1,

2

1

가

7

(n=7),

2

가

3

(n=6),

3

가

2

(n=6),

4

가

3

(n=18)

(detection accuracy)

가

2

15

, 1

5

3

2

(radiofrequency ablation)

receiver operating characteristic (ROC)

ROC

area zone (A_z)

2

10

(7)

(3)

(A_z)

Hanley and McNeil method

(14).

Wilcoxon's signed rank test

15

6

CT

9

(- fetoprotein)

MR

1.5 Tesla

GE Signa MR/I

CT

69

(General Electrics, Milwaukee, WI, U.S.A.)

0.7 - 4.2 cm

1.7 cm

T1 -

(TR=140 msec, TE=4

10 - 23

13

40

msec, =80,

=8 mm)

37

0.8 - 13.1

Mn - DPDP

cm

3.2 cm

,

14

20

(15),

T2 -

1

63 (91.3%)

(TR=4,000 msec, TE=90 msec,

=8 mm, ETL=12)

31 (83.8%)

,

2

56 (81.2%)

30 (81.1%)

MR

T1 -

,

12

T1 -

. Mn - DPDP

T1 -

18 -

가

(Table 1).

MR

38

27

Mn - DPDP Teslascan (Amersham Health, Oslo, Norway) 0.5 ml/kg 3 ml

가

1 2 52 (82.5%) 15 (21.7%) (Fig. 1).
 49 (87.5%) , 20 (64.5%)
 14 (46.7%) . 16 (23.2%),
 1 2 가 가 28
 11 (17.5%) 7 (12.5%) , 11 (40.6%) (Fig. 2) .
 (35.5%) 16 (53.3%) , 가 가 10 (14.5%)
 MR 가 가 15 (21.7%) .
 (Table 2).
 Mn - DPDP 가 37 36 (97.3%)
 69 44 , 1 (2.7%) (Fig. 3) ,
 (63.8%), 25 (36.2%) , 1 (2.7%) ,
 16
 (23.2%),
 38 (55.1%),

Table 1. Detection Accuracy in Liver Metastases and Hepatocellular Carcinomas

		Early (95% CI of Area)	Delay (95% CI of Area)	p value
Reader 1	Mets (<i>n</i> = 69)	0.917 (0.860 - 0.973)	0.912 (0.855 - 0.969)	> 0.1
	HCC (<i>n</i> = 37)	0.895 (0.809 - 0.980)	0.910 (0.827 - 0.992)	> 0.1
Reader 2	Mets (<i>n</i> = 69)	0.723 (0.616 - 0.831)	0.684 (0.565 - 0.803)	> 0.1
	HCC (<i>n</i> = 37)	0.624 (0.482 - 0.766)	0.715 (0.580 - 0.851)	> 0.1

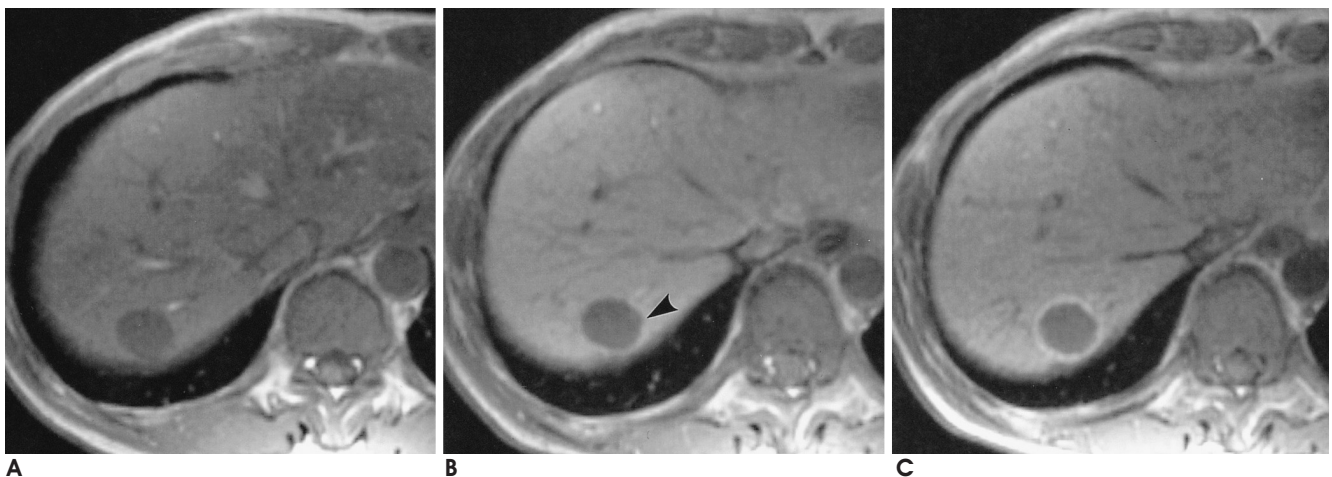
Mets: metastases, HCC: hepatocellular carcinomas, CI: confidence interval

Table 2. Comparison of Lesion Conspicuity between Mn-DPDP enhanced Early and Delay MR Images

		Early > Delay	Early = Delay	Early < Delay	p value
Reader 1	Mets (<i>n</i> = 63)	0	52	11	< 0.001
	HCC (<i>n</i> = 31)	0	20	11	< 0.001
Reader 2	Mets (<i>n</i> = 56)	0	49	7	< 0.01
	HCC (<i>n</i> = 30)	0	14	16	< 0.001

Mets: metastases, HCC: hepatocellular carcinomas

Wilcoxon 's signed rank test

**Fig. 1.** A 70-year-old man with liver metastasis from colon cancer.

Precontrast T1-weighted MR image (**A**) shows a 2.5 cm hypointense metastatic mass in segment VII of liver, which reveals thin and faint ring enhancement (arrowhead) on Mn-DPDP-enhanced early MR image (**B**). On postcontrast delay MR image (**C**), more prominent and thicker ring enhancement is demonstrated in the periphery of the metastatic mass.

: Mangafodipir Trisodium MR 가?

가 , (8).

(Table Gd - DTPA Mn - DPDP 가

3). MR

가 (5, 6, 16,

17).

Mn - DPDP 20 가

가 (6, 15), T1 - 가 (6). Mn - DPDP

가 (islet cell tumor)

Table 3. Comparison of Ring Enhancement Grade between Mn-DPDP enhanced Early and Delay MR Images

		Early > Delay	Early = Delay	Early < Delay	p value
Reader 1	Mets (n = 63)	0	21	42	< 0.001
	HCC (n = 31)				NA
Reader 2	Mets (n = 56)	0	20	36	< 0.001
	HCC (n = 30)	0	28	2	> 0.1

Mets: metastases, HCC: hepatocellular carcinomas, NA: not available, Wilcoxon 's signed rank test

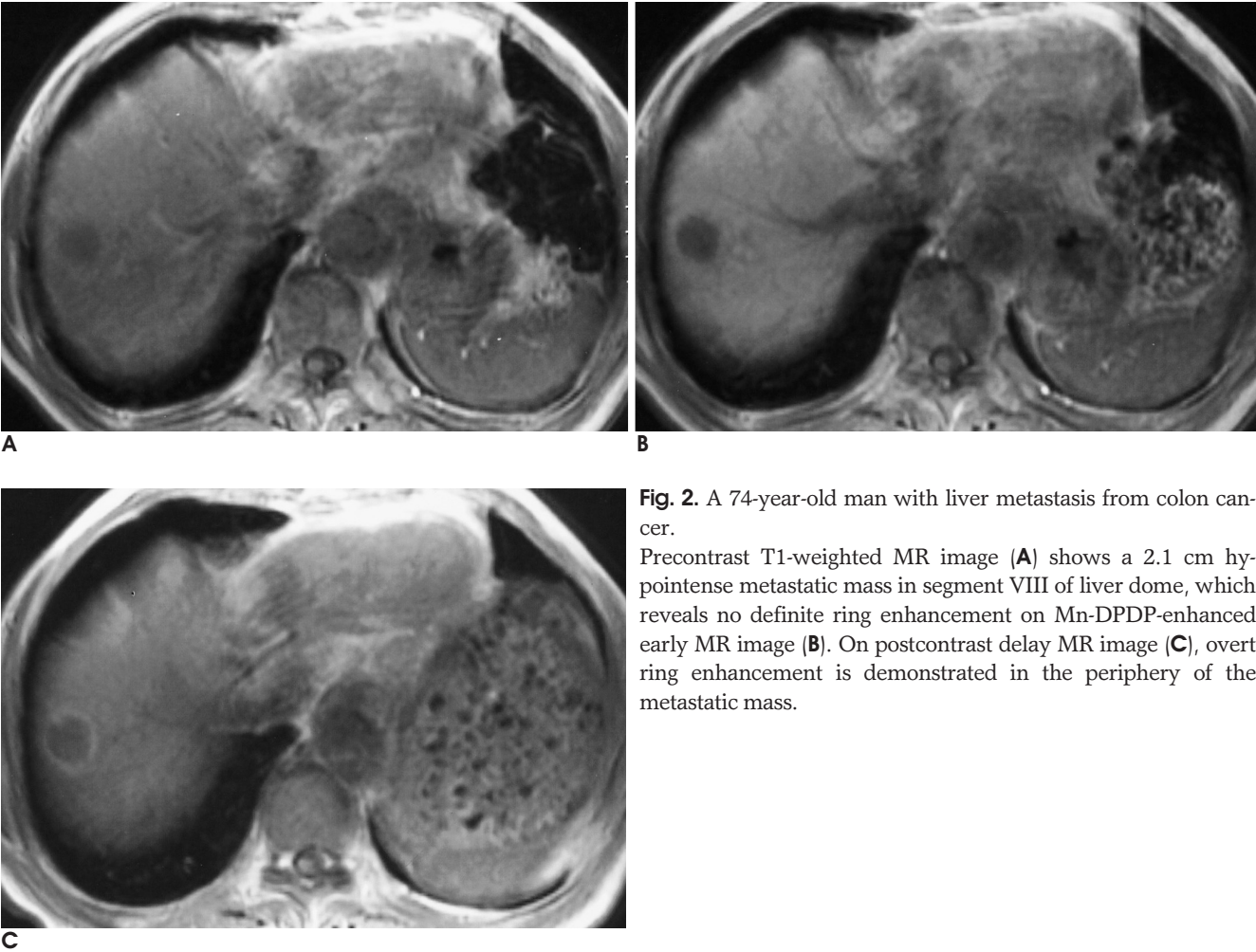


Fig. 2. A 74-year-old man with liver metastasis from colon cancer. Precontrast T1-weighted MR image (A) shows a 2.1 cm hypointense metastatic mass in segment VIII of liver dome, which reveals no definite ring enhancement on Mn-DPDP-enhanced early MR image (B). On postcontrast delay MR image (C), overt ring enhancement is demonstrated in the periphery of the metastatic mass.

(18 - 20).

63 (91.3%) 56 (81.2%),
31 (83.8%) 30 (81.1%)
, 가

가

가

가

CT

가 가 가 ,

. CT

CT

CT

가 가 CT

MR

Gd - DTPA

MR

(8, 21, 22).

CT

Gd - DTPA

MR

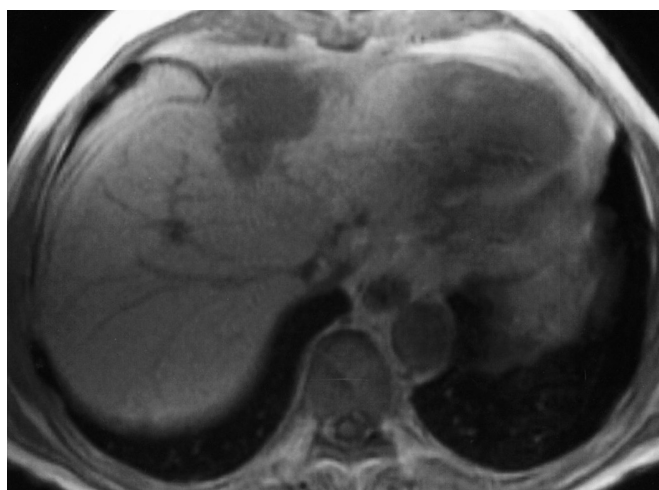
Mn - DPDP

MR

(12, 13)

12

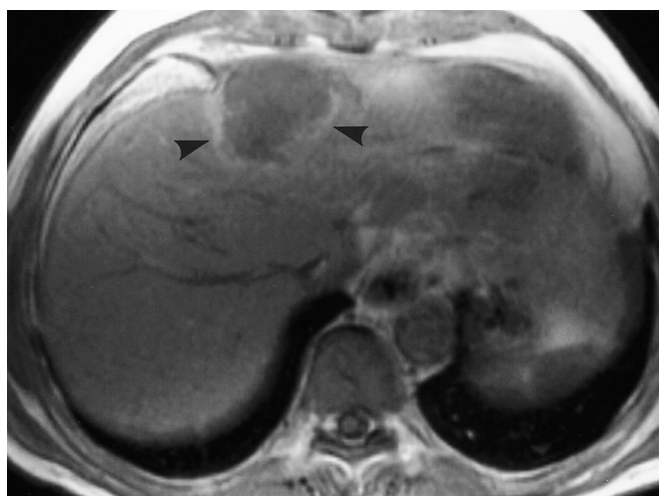
Mn - DPDP



A



B



C

Fig. 3. A 56-year-old man with hepatocellular carcinoma (HCC). Precontrast T1-weighted MR image (A) shows a 5.2 cm lobulated and hypointense HCC in segment IV of liver, which reveals slightly irregular ring enhancement (arrowheads) on Mn-DPDP-enhanced early MR image (B). On postcontrast delay MR image (C), an irregular ring enhancement (arrowheads) is still demonstrated in the periphery of the metastatic mass without interval change.

T1 -
가
(23).
가
, 24 가
(7, 11, 12).
Mn - DPDP
CT Gd - DTPA
MR 가
37 1 가
CT 가
Gd - DTPA
Mn - DPDP
(10, 24). CT
가
Gd - DTPA Mn - DPDP MR 가
Gd - DTPA
가 , Mn - DPDP
(21,
25, 26). 가
6 (30.0%),
9 (60.0%)
(
)
Mn - DPDP MR 12

1. Earls JP, Bluemke DA. New MR imaging contrast agents. *Magn Reson Imaging Clin N Am* 1999;7:255-273
2. Young SW, Simpson BB, Ratner AV, Matkin C, Carter EA. MRI measurement of hepatocyte toxicity using the new MRI contrast agent manganese dipyradoxal diphosphate, a manganese/pyradoxal 5-phosphate chelate. *Magn Reson Med* 1989;10:1-13
3. Jung G, Heindel W, Krahe T, Kugel H, Walter C, Fischbach R, et al. Influence of the hepatobiliary contrast agent mangafodipir trisodium (MN-DPDP) on the imaging properties of abdominal organs. *Magn Reson Imaging* 1998;16:925-931
4. Ni Y, Marchal G. Enhanced magnetic resonance imaging for tissue characterization of liver abnormalities with hepatobiliary contrast agents: an overview of preclinical animal experiments. *Top Magn Reson Imaging* 1998;9:183-195
5. Helmberger T, Semelka RC. New contrast agents for imaging the liver. *Magn Reson Imaging Clin N Am* 2001;9:745-766
6. Hahn PF, Saini S. Liver-specific MR imaging contrast agents. *Radiol Clin North Am* 1998;36:287-297
7. Liou J, Lee JK, Borrello JA, Brown JJ. Differentiation of hepatomas from nonhepatomatous masses: use of Mn-DPDP-enhanced MR images. *Magn Reson Imaging* 1994;12:71-79
8. Helmberger TK, Laubenberger J, Rummeny E, Jung G, Sievers K, Dohring W, et al. MRI characteristics in focal hepatic disease before and after administration of Mn-DPDP: discriminant analysis as a diagnostic tool. *Eur Radiol* 2002;12:62-70
9. Marti-Bonmati L, Lonjedo E, Poyatos C, Casillas C. Mn-DPDP enhancement characteristics and differentiation between cirrhotic and noncirrhotic livers. *Invest Radiol* 1998;33:717-722
10. King LJ, Burkill GJ, Scurr ED, Vlavianos P, Murray-Lyons I, Healy JC. Mn-DPDP enhanced magnetic resonance imaging of focal liver lesions. *Clin Radiol* 2002;57:1047-1057
11. Coffin CM, Diche T, Mahfouz A, Alexandre M, Caseiro-Alyes F, Rahmouni A, et al. Benign and malignant hepatocellular tumors: evaluation of tumoral enhancement after mangafodipir trisodium injection on MR imaging. *Eur Radiol* 1999;9: 444-449
12. Kane PA, Ayton V, Walters L, Benjamin I, Heaton ND, Williams R, et al. Mn-DPDP-enhanced MR imaging of the liver. Correlation with surgical findings. *Acta Radiol* 1997;38:650-654
13.

Gadolinium chelate	Mangafodipir trisodium
:	.
2002;46:561-567	
14. Hanley JA, McNeil BJ. A method of comparing the areas under receiver operating characteristic curves derived from the same cases. *Radiology* 1983;148:839-843
15. Rummeny EJ, Marchal G. Liver imaging. Clinical applications and future perspectives. *Acta Radiol* 1997;38:626-630
16. Semelka RC, Worawattanakul S, Kelekis NL, John G, Woosley JT, Graham M, et al. Liver lesion detection, characterization, and effect on patient management: comparison of single-phase spiral CT and current MR techniques. *J Magn Reson Imaging* 1997;7:1040-1047
17. Kettritz U, Schlund JF, Wilbur K, Eisenberg LB, Semelka RC. Comparison of gadolinium chelates with manganese-DPDP for liver lesion detection and characterization: preliminary results. *Magn Reson Imaging* 1996;14:1185-1190
18. Wang C, Ahlstrom H, Eriksson B, Lonnemark M, McGill S, Hemmingsson A. Uptake of mangafodipir trisodium in liver

- metastases from endocrine tumors. *J Magn Reson Imaging* 1998;8: 682-686
19. Kettritz U, Semelka RC. Contrast-enhanced MR imaging of the pancreas. *Magn Reson Imaging Clin N Am* 1996;4:87-100
 20. Mathieu D, Coffin C, Kobeiter H, Casciro-Alves F, Mahfouz A, Rahmouni A, et al. Unexpected MR-T1 enhancement of endocrine liver metastases with mangafodipir. *J Magn Reson Imaging* 1999;10:193-195
 21. Martin DR, Semelka RC. Imaging of benign and malignant focal liver lesions. *Magn Reson Imaging Clin N Am* 2001;9:785-802
 22. Pedro MS, Semelka RC, Braga L. MR imaging of hepatic metastases. *Magn Reson Imaging Clin N Am* 2002;10:15-29
 23. Semelka RC, Hussain SM, Marcos HB, Woosley JT. Perilesional enhancement of hepatic metastases: correlation between MR imaging and histopathologic findings-initial observations. *Radiology* 2000;215: 89-94
 24. Oudkerk M, Torres CG, Song B, Konig M, Grimm J, Fernandez-Cuadrado J, et al. Characterization of liver lesions with mangafodipir trisodium-enhanced MR imaging: multicenter study comparing MR and dual-phase spiral CT. *Radiology* 2002;223:517-524
 25. Martin DR, Semelka RC, Chung JJ, Balci NC, Wilber K. Sequential use of gadolinium chelate and mangafodipir trisodium for the assessment of focal liver lesions: Initial observations. *Magn Reson Imaging* 2000; 18:955-963
 26. Sahani DV, O'Malley ME, Bhat S, Hahn PF, Saini S. Contrast-enhanced MRI of the liver with mangafodipir trisodium: imaging technique and results. *J Comput Assist Tomogr* 2002;26:216-222

J Korean Radiol Soc 2004;51:299 - 305

Are the Delay Images Necessary to Evaluate the Liver Metastatic Lesions on Mangafodipir Trisodium Enhanced Liver MRI?: Comparison with Hepatocellular Carcinomas¹

Jae-Joon Chung, M.D.^{1,2}, Hee Chul Yang, M.D.², Myeong-Jin Kim, M.D.,
Jong Tae Lee, M.D., Hyung Sik Yoo, M.D., Ki Whang Kim, M.D.

¹Department of Diagnostic Radiology, Yonsei University College of Medicine, Research Institute of Radiological Science, Yonsei University

²Department of Diagnostic Radiology, NHIC Ilsan Hospital

Purpose: To assess whether ring enhancements of liver metastases on Mn-DPDP enhanced, early MR images were well visualized on delayed images, as compared with those of hepatocellular carcinomas (HCC), and to investigate the detection accuracy and conspicuity of each tumor.

Materials and Methods: Twenty patients with liver metastases and 15 with HCC were studied by Mn-DPDP enhanced, T1-weighted MR images. Peripheral ring enhancement and conspicuity were investigated. Differences in detection accuracy and frequency of ring enhancement in liver metastases and HCC were assessed.

Results: In liver metastases ($n=69$), 44 cases (63.8%) without ring enhancement and 25 (36.2%) with were noted on early images. Sixteen cases (23.2%) without ring enhancement, 38 (55.1%) with ring enhancement similar to the early images, and 15 (21.7%) with prominent ring enhancement were noted on delayed images. In HCC ($n=37$), 36 cases (97.3%) without ring enhancement and 1 case (2.7%) with were noted on early images. There was no difference of detection accuracy in liver metastases or HCC between the 2 readings. Ring enhancement and conspicuity of each tumor were superior on delayed images. Ring enhancement in liver metastases was better seen on delayed images.

Conclusion: Ring enhancement in liver metastases was well presented on Mn-DPDP enhanced, delayed MR images, which was useful to differentiate liver metastases from HCC.

Index words : Liver, neoplasms

Liver, MR

Magnetic resonance (MR)

Magnetic resonance (MR), contrast enhancement

Address reprint requests to : Jae-Joon Chung, M.D., Department of Diagnostic Radiology, YUMC,
134 Shinchon-dong, Seodaemun-gu, Seoul 120-752, Korea.
Tel. 82-2-361-5837 Fax. 82-2-393-3035 E-mail: jjchung@yumc.yonsei.ac.kr